Monin–Obukhov Similarity and Local-Free-Convection Scaling in the Atmospheric Boundary Layer Using Matched Asymptotic Expansions

CHENNING TONG AND MENGJIE DING

Department of Mechanical Engineering, Clemson University, Clemson, South Carolina

(Manuscript received 12 January 2018, in final form 28 June 2018)

ABSTRACT

The Monin–Obukhov similarity theory (MOST) is the foundation for understanding the atmospheric surface layer. It hypothesizes that nondimensional surface-layer statistics are functions of z/L only, where z and L are the distance from the ground and the Obukhov length, respectively. In particular, it predicts that in the convective surface layer, local free convection (LFC) occurs at heights $-z/L \gg 1$ and $z/z_i \ll 1$, where z_i is the inversion height. However, as a hypothesis, MOST is based on phenomenology. In this work we derive MOST and the LFC scaling from the equations for the velocity and potential temperature variances using the method of matched asymptotic expansions. Our analysis shows that the dominance of the buoyancy and shear production in the outer ($-z/L \gg 1$) and inner ($-z/L \lesssim 1$) layers, respectively, results in a nonuniformly valid solution and a singular perturbation problem and that $-L$ is the thickness of the inner layer. The inner solutions are found to be functions of z/L only, providing a proof of MOST for the vertical velocity and potential temperature variances. Matching between the inner and outer solutions results in the LFC scaling. We then obtain the corrections to the LFC scaling near the edges of the LFC region ($-z/L \sim 1$ and $z/z_i \sim 1$). The nondimensional coefficients in the expansions are determined using measurements. The resulting composite expansions provide unified expressions for the variance profiles in the convective atmospheric surface layer and show very good agreement with the data. This work provides strong analytical support for MOST.

1. Introduction

The Monin–Obukhov similarity theory (MOST; Monin and Obukhov 1954; Obukhov 1946) is the foundation for our understanding of the atmospheric surface layer. It hypothesizes that the surface-layer ($z \ll z_i$) dynamics is governed by the kinematic surface stress (the square of the friction velocity) u_*^2, the surface temperature flux Q, the buoyancy parameter β, and the height from the surface z, where z_i is the boundary layer (inversion) height. Any nondimensional statistics therefore is a function of z/L, where $L = -u_*^3/(\kappa\beta Q)$ is the Obukhov length, and κ is the von Kármán constant. The theory predicts that for $-z/L < 1$, the shear production of the turbulent kinetic energy dominates, and for $-z/L > 1$, the buoyancy production dominates. In particular, it predicts that for the special case of $-z/L \gg 1$ (but $z/z_i \ll 1$), the influence of mean shear becomes negligible, resulting in the so-called local-free-convection (LFC) scaling (Tennekes 1970; Wyngaard et al. 1971). In this layer the vertical velocity and potential temperature variances do not depend on u_*, and have the forms $\overline{w^2} \sim (\beta Q z)^{2/3}$ and $\overline{\theta^2} \sim Q^{4/3}(\beta z)^{-2/3}$, respectively. However, when the conditions $-z/L \gg 1$ and $z/z_i \ll 1$ are not satisfied (e.g., $-z/L \sim 1$ or $z/z_i \sim 1$), we expect departure from the LFC scaling (Wyngaard et al. 1971). Field measurements support the prediction for the vertical velocity and potential temperature variances (section 3e).

While MOST has been successfully used in predicting the surface-layer scaling, it is nevertheless a hypothesis based largely on the phenomenology of the surface layer and dimensional arguments. Measurements can provide support to MOST, but it cannot positively prove it. In the present study, we derive MOST and the LFC scaling from first principles using the equations for the velocity and potential temperature variances and the method of matched asymptotic expansions (Bender and Orszag 1978; Van Dyke 1975; Cousteix and Mauss 2007). We also derive from the expansions the corrections to account for the departure from the LFC scaling for $-z/L \sim 1$ or $z/z_i \sim 1$. The composite expansions include the influence of both $-z/L$ and $-z_i/L$ and are based on the physics of the surface layer. The former is an approximation of the Monin–Obukhov

Corresponding author: Prof. Chenning Tong, ctong@clemson.edu

DOI: 10.1175/JAS-D-18-0016.1

functions near $-z/L \sim 1$, whose functional forms cannot be obtained analytically from dimensional analysis. Instead they must be obtained empirically from observations. The influence of $-z_i/L$ is absent in MOST. Thus, the derivation is a major step toward an analytical proof of MOST. The analytical prediction of the variance profiles can benefit numerical weather prediction models under convective conditions. It will also be important for modeling atmospheric dispersion.

In the following we first examine the variance equations for the velocity components and potential temperature to identify the mathematical structure of the problem (a singular perturbation problem). We then perform the method of matched asymptotic expansions to obtain MOST and the LFC scaling as well as the corrections to the latter for $-z/L \sim 1$ or $z/z_i \sim 1$. The analytical results for LFC are then compared with measurements and are followed by the conclusions.

2. The mathematical structure of the problem

The equations for the velocity components and potential temperature variances in a horizontally homogeneous atmospheric boundary layer are (e.g., Wyngaard and Coté 1971)

$$\frac{1}{2}\frac{\partial \overline{w^2}}{\partial t} = -\frac{1}{2}\frac{\partial \overline{w^3}}{\partial z} + \overline{p\frac{\partial w}{\partial z}} - \frac{\partial \overline{pw}}{\partial z} + \frac{g}{T}\overline{w\theta} - \varepsilon_3, \quad (1)$$

$$\frac{1}{2}\frac{\partial \overline{u^2}}{\partial t} = -\overline{uw}\frac{\partial U}{\partial z} - \frac{1}{2}\frac{\partial \overline{wu^2}}{\partial z} + \overline{p\frac{\partial u}{\partial x}} - \varepsilon_1, \quad (2)$$

$$\frac{1}{2}\frac{\partial \overline{v^2}}{\partial t} = -\frac{1}{2}\frac{\partial \overline{wv^2}}{\partial z} + \overline{p\frac{\partial v}{\partial y}} - \varepsilon_2, \quad \text{and} \quad (3)$$

$$\frac{1}{2}\frac{\partial \overline{\theta^2}}{\partial t} = -\overline{w\theta}\frac{\partial \Theta}{\partial z} - \frac{1}{2}\frac{\partial \overline{w\theta^2}}{\partial z} - \varepsilon_\theta, \quad (4)$$

where ε_1, ε_2, ε_3, and ε_θ are dissipation rates for $\overline{u^2}/2$, $\overline{v^2}/2$, $\overline{w^2}/2$, and $\overline{\theta^2}/2$, respectively; and p is the kinematic pressure. The upper- and lowercase letters denote the mean and fluctuating variables, respectively. The mean wind is aligned with the U direction. When the shear production is absent (free convection), Eqs. (1)–(4) have the mixed-layer scaling; therefore, the resulting nondimensional solution depends on the nondimensional independent variable z/z_i:

$$\frac{\overline{w^2}}{w_*^2} = \overline{w_o^2}\left(\frac{z}{z_i}\right), \quad \frac{\overline{u^2}}{w_*^2} = \overline{u_o^2}\left(\frac{z}{z_i}\right),$$

$$\frac{\overline{v^2}}{w_*^2} = \overline{v_o^2}\left(\frac{z}{z_i}\right), \quad \frac{\overline{\theta^2}}{(Q/w_*)^2} = \overline{\theta_o^2}\left(\frac{z}{z_i}\right), \quad (5)$$

where $w_* = (\beta Q z_i)^{1/3}$ is the mixed-layer velocity scale. The subscript o will be used to denote the outer variables defined in the next section. The mixed-layer scaling also holds in the presence of the mean shear production for $z \gg -L$, since the effects of the shear production (of $\overline{u^2}$) are small within this range of heights. Note that the terms in the $\overline{u^2}$ and $\overline{v^2}$ equations acquire the mixed-layer scaling (except the shear production term) as a result of the pressure–strain-rate correlation. However, the solutions in Eq. (5) are not valid for $-z/L \lesssim 1$, where the shear production, which has the surface-layer scaling (as a result of the parameters u_* and z), becomes a leading term in Eq. (2); that is, the presence of the shear production term results in a nonuniformly valid solution. This shear-production-dominated layer always exists, as long as it is above the roughness layer, for any small but nonzero mean shear. Therefore, zero mean shear is a singular limit for the solution; that is, the structure of the solution for a case with the mean shear approaching zero (but not equal to zero) is fundamentally different from that with the mean shear equaling zero. Consequently, the system described by Eqs. (1)–(4) has the structure of a singular perturbation problem, whose solution can be obtained using the method of matched asymptotic expansions. The layers with $-z/L \gg 1$ and $-z/L \lesssim 1$ are the so-called outer and inner layers, respectively.

3. Matched asymptotic expansions

In this section we use the method of matched asymptotic expansions to solve the singular perturbation problem to derive MOST and the LFC scaling for the vertical velocity (the horizontal components do not have this scaling) and potential temperature variances, as well as to obtain the second-order corrections to the LFC scaling. Matched asymptotic expansions are a method to solve a set of differential equations having a solution that has different scaling in different parts of the solution domain, that is, a nonuniformly valid solution. In this study they are the mixed-layer scaling and surface-layer scaling. The solution in each part of the domain is expressed as series expansions with their respective scaling. The expansions in the different parts are then asymptotically matched to obtain composite expansions (uniformly valid solution).

a. Outer expansions

We define the dimensionless outer variables in the singular perturbation problem $\overline{w_o^2}$, $\overline{u_o^2}$, $\overline{v_o^2}$, $\overline{\theta_o^2}$, $(\partial\Theta/\partial z)_o$, z_o, p_o, $\overline{w\theta}_o$, $\overline{w\theta^2}_o$, and τ using the mixed-layer scales as follows:

$$\overline{w^2} = w_*^2\overline{w_o^2}, \quad \overline{u^2} = w_*^2\overline{u_o^2}, \quad \overline{v^2} = w_*^2\overline{v_o^2}, \quad \overline{\theta^2} = \left(\frac{Q}{w_*}\right)^2\overline{\theta_o^2},$$

$$\frac{\partial\Theta}{\partial z} = \frac{Q}{w_* z_i}\left(\frac{\partial\Theta}{\partial z}\right)_o, \quad z = z_i z_o, \quad p = w_*^2 p_o,$$

$$\overline{w\theta} = Q\overline{w\theta}_o, \quad \overline{w\theta^2} = \left(\frac{Q}{w_*}\right)^2 w_*\overline{w\theta^2}_o, \quad t = \frac{z_i}{w_*}\tau. \quad (6)$$

The nondimensional forms of Eqs. (1), (2), and (4) in terms of the outer variables are

$$\frac{1}{2}\frac{\partial\overline{w_o^2}}{\partial\tau}=-\frac{1}{2}\frac{\partial\overline{w_o^3}}{\partial z_o}+\left(\overline{p\frac{\partial w}{\partial z}}\right)_o-\left(\frac{\partial\overline{pw}}{\partial z}\right)_o+\overline{w\theta}_o-\varepsilon_{3o}, \tag{7}$$

$$\frac{1}{2}\frac{\partial\overline{u_o^2}}{\partial\tau}=-\overline{uw}\frac{\partial U}{\partial z}\frac{z_i}{w_*^3}-\frac{1}{2}\frac{\partial\overline{w_ou_o^2}}{\partial z_o}+\left(\overline{p\frac{\partial u}{\partial x}}\right)_o-\varepsilon_{1o},\quad\text{and} \tag{8}$$

$$\frac{1}{2}\frac{\partial\overline{\theta_o^2}}{\partial\tau}=-\overline{w\theta}_o\left(\frac{\partial\Theta}{\partial z}\right)_o-\frac{1}{2}\frac{\partial\overline{w\theta^2}_o}{\partial z_o}-\varepsilon_{\theta o}. \tag{9}$$

For convenience, the equation for $\overline{v_o^2}$ is not given, as it is not explicitly used in the analysis. In the outer layer, the buoyancy production term and the pressure–strain-rate terms are of order one (leading terms), while the nondimensional shear production term $-\overline{uw}(\partial U/\partial z)(z_i/w_*^3)<(u_*^3/z)(z_i/w_*^3)\ll 1$; therefore, it is a second-order term and can be written as

$$-\overline{uw}\frac{\partial U}{\partial z}\frac{z_i}{w_*^3}=\epsilon\overline{uw}_o\left(\frac{\partial U}{\partial z}\right)_o, \tag{10}$$

where ϵ is a small parameter whose order of magnitude has yet to be determined. However, it will become a leading term when z is sufficiently small, and therefore results in a nonuniformly valid solution and a singular perturbation problem. Unlike this shear production term, the production of $\overline{\theta_o^2}$ in Eq. (9) is a leading term and therefore is not the source of singularity as $z_o\to 0$.

The outer expansions of the velocity components and potential temperature and their variances in terms of the power of ϵ can be written as

$$\begin{aligned}&w_o(z_o)=w_{o,1}(z_o)+\epsilon w_{o,2}(z_o)+O(\epsilon^2),\\&u_o(z_o)=u_{o,1}(z_o)+\epsilon u_{o,2}(z_o)+O(\epsilon^2),\quad\text{and}\\&\theta_o(z_o)=\theta_{o,1}(z_o)+\epsilon\theta_{o,2}(z_o)+O(\epsilon^2),\end{aligned} \tag{11}$$

$$\begin{aligned}&\overline{w_o^2}(z_o)=\overline{w_{o,1}^2}(z_o)+2\epsilon\overline{w_{o,1}(z_o)w_{o,2}(z_o)}+O(\epsilon^2),\\&\overline{u_o^2}(z_o)=\overline{u_{o,1}^2}(z_o)+2\epsilon\overline{u_{o,1}(z_o)u_{o,2}(z_o)}+O(\epsilon^2),\quad\text{and}\\&\overline{\theta_o^2}(z_o)=\overline{\theta_{o,1}^2}(z_o)+2\epsilon\overline{\theta_{o,1}(z_o)\theta_{o,2}(z_o)}+O(\epsilon^2).\end{aligned} \tag{12}$$

The equations for the leading-order terms $\overline{w_{o,1}^2}$, $\overline{u_{o,1}^2}$, and $\overline{\theta_{o,1}^2}$ are obtained by substituting Eqs. (11) and (12) into Eqs. (7), (8), and (9) and collecting terms of order one (ϵ^0).

b. Inner expansions and a proof of MOST

As discussed above, when z is sufficiently small (in the inner layer), the term containing the mean shear in Eq. (8) becomes a leading term and the outer solution is no longer valid. A new scaling is needed in the inner layer. We define the dimensionless inner variables $\overline{w_{\rm in}^2}$, $\overline{u_{\rm in}^2}$, $\overline{\theta_{\rm in}^2}$, $(\partial\Theta/\partial z)_{\rm in}$, $z_{\rm in}$, $p_{\rm in}$, $\overline{w\theta}_{\rm in}$, and $\overline{w\theta^2}_{\rm in}$ as follows:

$$\begin{aligned}&\overline{w^2}=u_*^2\overline{w_{\rm in}^2},\quad\overline{u^2}=u_*^2\overline{u_{\rm in}^2},\quad\overline{\theta^2}=\left(\frac{Q}{u_*}\right)^2\overline{\theta_{\rm in}^2},\\&\frac{\partial\Theta}{\partial z}=\frac{Q}{u_*L'}\left(\frac{\partial\Theta}{\partial z}\right)_{\rm in},\quad z=L'z_{\rm in},\quad p=u_*^2p_{\rm in},\\&\overline{w\theta}=Q\overline{w\theta}_{\rm in},\quad\overline{w\theta^2}=\left(\frac{Q}{u_*}\right)^2u_*\overline{w\theta^2}_{\rm in},\end{aligned} \tag{13}$$

where L' is the inner length scale (thickness of the inner layer) and has yet to be determined. Here u_* is used as the velocity scale, as shown in the derivation of the multipoint Monin–Obukhov similarity (MMO; Tong and Nguyen 2015; Tong and Ding 2018, manuscript submitted to *J. Fluid Mech.*). The nondimensional forms of Eqs. (1), (2), and (4) in terms of the inner variables are

$$\begin{aligned}\frac{1}{2}\frac{u_*^2w_*}{z_i}\frac{\partial\overline{w_{\rm in}^2}}{\partial\tau}=&-\frac{1}{2}\frac{\partial\overline{w_{\rm in}^3}}{\partial z_{\rm in}}\frac{u_*^3}{L'}+\left(\overline{p\frac{\partial w}{\partial z}}\right)_{\rm in}\frac{u_*^3}{L'}\\&-\left(\frac{\partial\overline{pw}}{\partial z}\right)_{\rm in}\frac{u_*^3}{L'}+\frac{g}{T}Q\overline{w\theta}_{\rm in}-\varepsilon_{3\rm in}\frac{u_*^3}{L'},\end{aligned} \tag{14}$$

$$\begin{aligned}\frac{1}{2}\frac{u_*^2w_*}{z_i}\frac{\partial\overline{u_{\rm in}^2}}{\partial\tau}=&-\overline{uw}_{\rm in}\left(\frac{\partial U}{\partial z}\right)_{\rm in}\frac{u_*^3}{L'}-\frac{1}{2}\frac{\partial\overline{w_{\rm in}u_{\rm in}^2}}{\partial z_{\rm in}}\frac{u_*^3}{L'}\\&+\left(\overline{p\frac{\partial u}{\partial x}}\right)_{\rm in}\frac{u_*^3}{L'}-\varepsilon_{1\rm in}\frac{u_*^3}{L'},\quad\text{and}\end{aligned} \tag{15}$$

$$\begin{aligned}\frac{1}{2}\left(\frac{Q}{u_*}\right)^2\frac{w_*}{z_i}\frac{\partial\overline{\theta_{\rm in}^2}}{\partial\tau}=&-Q\frac{Q}{u_*L'}\overline{w\theta}_{\rm in}\left(\frac{\partial\Theta}{\partial z}\right)_{\rm in}\\&-\frac{1}{2}\left(\frac{Q}{u_*}\right)^2\frac{u_*}{L'}\frac{\partial\overline{w\theta^2}_{\rm in}}{\partial z_{\rm in}}-\varepsilon_{\theta\rm in}\frac{Q^2}{u_*L'}.\end{aligned} \tag{16}$$

In the inner layer $z\lesssim L'$, $-\overline{uw}(\partial U/\partial z)$ needs to be a leading-order term; thus, it must scale as

$$-\overline{uw}\frac{\partial U}{\partial z}\sim u_*^2\frac{u_*}{L'}\sim\overline{p\frac{\partial u}{\partial x}}\sim\overline{p\frac{\partial w}{\partial z}}\sim\frac{g}{T}Q\overline{w\theta}_{\rm in}, \tag{17}$$

leading to $gQ/T\sim u_*^3/L'$. The fact that the pressure–strain-rate correlation terms are of the same order of magnitude and are leading-order terms in both the $\overline{u_{\rm in}^2}$ and $\overline{w_{\rm in}^2}$ equations is used in deriving Eq. (17). Therefore, the inner length scale L' is the Obukhov length. Equations (14), (15), and (16) become

$$\frac{1}{2}\epsilon'\frac{\partial\overline{w_{\rm in}^2}}{\partial\tau}=-\frac{1}{2}\frac{\partial\overline{w_{\rm in}^3}}{\partial z_{\rm in}}+\left(\overline{p\frac{\partial w}{\partial z}}\right)_{\rm in}-\left(\frac{\partial\overline{pw}}{\partial z}\right)_{\rm in}+\overline{w\theta}_{\rm in}-\varepsilon_{3\rm in}, \tag{18}$$

$$\frac{1}{2}\epsilon'\frac{\partial\overline{u_{\rm in}^2}}{\partial\tau} = -\overline{uw}_{\rm in}\left(\frac{\partial U}{\partial z}\right)_{\rm in} - \frac{1}{2}\frac{\partial\overline{w_{\rm in}u_{\rm in}^2}}{\partial z_{\rm in}} + \overline{\left(p\frac{\partial u}{\partial x}\right)}_{\rm in} - \varepsilon_{1\rm in}\,, \tag{19}$$

and

$$\frac{1}{2}\epsilon'\frac{\partial\overline{\theta_{\rm in}^2}}{\partial\tau} = -\overline{w\theta}_{\rm in}\frac{\partial\Theta_{\rm in}}{\partial z_{\rm in}} - \frac{1}{2}\frac{\partial\overline{w\theta^2}_{\rm in}}{\partial z_{\rm in}} - \varepsilon_{\theta\rm in}\,, \tag{20}$$

where

$$\epsilon' = -\frac{L}{z_i}\frac{w_*}{u_*} = \kappa^{-1/3}\left(-\frac{z_i}{L}\right)^{-2/3}, \tag{21}$$

is a small parameter. We note that for the vertical velocity and temperature variances to follow MOST—that is, to be Monin–Obukhov (M-O) similar, and to have a solution that scales with the inner variables—the variance equations must also be M-O similar. Although the horizontal velocity variances have mixed-layer scaling and are not M-O similar, their rate equations are (or have apparent M-O similarity; Ding et al. 2018, manuscript submitted to *J. Fluid Mech.*; Tong and Ding 2018, manuscript submitted to *J. Fluid Mech.*). Therefore, the dynamics of the horizontal and vertical velocity components in the surface layer are M-O similar. We can therefore write the inner expansions for the vertical velocity and potential temperature variances as

$$\overline{w_{\rm in}^2}(z_{\rm in}) = \overline{w_{\rm in,1}^2}(z_{\rm in}) + 2\epsilon'\overline{w_{\rm in,1}(z_{\rm in})w_{\rm in,2}(z_{\rm in})} + O(\epsilon'^2)\,,$$
$$\overline{\theta_{\rm in}^2}(z_{\rm in}) = \overline{\theta_{\rm in,1}^2}(z_{\rm in}) + 2\epsilon'\overline{\theta_{\rm in,1}(z_{\rm in})\theta_{\rm in,2}(z_{\rm in})} + O(\epsilon'^2)\,. \tag{22}$$

The results in Eq. (22) are of fundamental importance: They show that the nondimensional vertical velocity and potential temperature variances are functions of z/L only, thus providing a proof of MOST for these variables.

c. Asymptotic matching to derive the LFC scaling

Since the outer and inner expansions describe the dynamics at the outer and inner scales, respectively, and are valid for $-z/L \gg 1$ and $z/z_i \ll 1$, there exists an overlapping region where both conditions are satisfied and the expansions represent the same function. Therefore, if we write the outer expansion as a function of the inner variable and the inner expansion as a function of the outer variable, they should be equal.

The inner expansion of the outer expansion of $\overline{w^2}$ is

$$\overline{w^2} = w_*^2\left[\overline{w_{o,1}^2}\left(-\frac{L}{z_i}z_{\rm in}\right) + 2\epsilon\overline{w_{o,1}\left(-\frac{L}{z_i}z_{\rm in}\right)w_{o,2}\left(-\frac{L}{z_i}z_{\rm in}\right)} + \cdots\right], \quad \text{as } \epsilon\to 0, \text{ with } z_{\rm in} \text{ fixed}$$
$$\sim u_*^2\left(-\frac{z_i}{L}\right)^{2/3}\overline{w_{o,1}^2}\left(-\frac{L}{z_i}z_{\rm in}\right), \quad \sim u_*^2\left(-\frac{z_i}{L}\right)^{2/3}\left(-\frac{L}{z_i}z_{\rm in}\right)^{\alpha}, \tag{23}$$

keeping only one term.

The outer expansion of the inner expansion of $\overline{w^2}$ is

$$\overline{w^2} = u_*^2\left[\overline{w_{\rm in,1}^2}\left(-\frac{z_i}{L}z_o\right) + 2\epsilon'\overline{w_{\rm in,1}\left(-\frac{z_i}{L}z_o\right)w_{\rm in,2}\left(-\frac{z_i}{L}z_o\right)} + \cdots\right], \quad \text{as } \epsilon'\to 0, \text{ with } z_o \text{ fixed}$$
$$\sim w_*^2\left(-\frac{L}{z_i}\right)^{2/3}\overline{w_{\rm in,1}^2}\left(-\frac{z_i}{L}z_o\right), \quad \sim u_*^2 z_{\rm in}^{\alpha}\,. \tag{24}$$

Matching Eqs. (23) and (24) results in $\alpha = 2/3$. Thus,

$$\overline{w^2} \sim w_*^2\left(\frac{z}{z_i}\right)^{2/3} \sim u_*^2\left(-\frac{z}{L}\right)^{2/3} = u_f^2\,. \tag{25}$$

This is the LFC scaling for the vertical velocity variance, and u_f is the velocity scale.

The inner expansion of the outer expansion of $\overline{\theta^2}$ is

$$\overline{\theta^2} = \left(\frac{Q}{w_*}\right)^2\left[\overline{\theta_{o,1}^2}\left(-\frac{L}{z_i}z_{\rm in}\right) + 2\epsilon\overline{\theta_{o,1}\left(-\frac{L}{z_i}z_{\rm in}\right)\theta_{o,2}\left(-\frac{L}{z_i}z_{\rm in}\right)} + \cdots\right], \quad \text{as } \epsilon\to 0, \text{ with } z_{\rm in} \text{ fixed}$$
$$\sim \left(\frac{Q}{u_*}\right)^2\left(-\frac{L}{z_i}\right)^{2/3}\overline{\theta_{o,1}^2}\left(-\frac{L}{z_i}z_{\rm in}\right), \quad \sim \left(\frac{Q}{u_*}\right)^2\left(-\frac{L}{z_i}\right)^{2/3}\left(-\frac{L}{z_i}z_{\rm in}\right)^{\gamma}, \tag{26}$$

keeping only one term.

The outer expansion of the inner expansion of $\overline{\theta^2}$ is

$$\overline{\theta^2} = \left(\frac{Q}{u_*}\right)^2 \left[\overline{\theta^2_{\mathrm{in},1}}\left(-\frac{z_i}{L}z_o\right) + 2\epsilon' \overline{\theta_{\mathrm{in},1}\left(-\frac{z_i}{L}z_o\right)\theta_{\mathrm{in},2}\left(-\frac{z_i}{L}z_o\right)} + \cdots\right], \quad \text{as } \epsilon' \to 0, \text{ with } z_o \text{ fixed}$$
$$\sim \left(\frac{Q}{w_*}\right)^2 \left(-\frac{z_i}{L}\right)^{2/3} \overline{\theta^2_{\mathrm{in},1}}\left(-\frac{z_i}{L}z_o\right), \quad \sim \left(\frac{Q}{u_*}\right)^2 z_{\mathrm{in}}^{\gamma}. \tag{27}$$

Matching Eqs. (26) and (27) results in $\gamma = -2/3$. Thus,

$$\overline{\theta^2_{o,1}} \sim \left(\frac{z}{z_i}\right)^{-2/3}. \tag{28}$$

This is the LFC scaling for the temperature variance.

d. Second-order corrections to the leading-order solutions (LFC scaling)

When the conditions for the overlapping region ($-z/L \gg 1$ and $z/z_i \ll 1$) are not satisfied, departures from the LFC scaling [Eqs. (25) and (28)] are expected. Corrections to account for the departures can be made by including the higher-order terms in the expansions in Eqs. (12) and (22). To obtain the second-order terms, we need to first determine the scaling of the shear production term $-\overline{uw}(\partial U/\partial z)$ and the small parameter ϵ. Since the surface layer is a "constant flux" layer (e.g., Haugen et al. 1971), the turbulent flux $\overline{uw}$ is approximately independent of height from the surface and scales as u_*^2. We consider the shear stress $\overline{uw}$ budget equation (e.g., Wyngaard et al. 1971),

$$\frac{\partial \overline{uw}}{\partial t} + \overline{w^2}\frac{\partial U}{\partial z} - \frac{g}{T}\overline{u\theta} + \frac{\partial \overline{uw^2}}{\partial z} + \overline{\frac{w\partial p}{\partial x}} + \overline{\frac{u\partial p}{\partial z}} = 0. \tag{29}$$

Nondimensionalizing $\overline{uw}$ by u_*^2, t by z/u_f, and $\overline{w^2}$ by u_f^2 results in

$$\frac{z}{u_f}\frac{1}{u_*^2}\frac{\partial \overline{uw}}{\partial t} + \frac{z}{u_f}\frac{1}{u_*^2}\overline{w^2}\frac{\partial U}{\partial z} + \frac{z}{u_f}\frac{1}{u_*^2}\left(-\frac{g}{T}\overline{u\theta} + \frac{\partial \overline{uw^2}}{\partial z} + \overline{\frac{w\partial p}{\partial x}} + \overline{\frac{u\partial p}{\partial z}}\right) = 0. \tag{30}$$

The shear production term must be a leading term [$O(1)$] in Eq. (29). Thus,

$$\frac{z}{u_f}\frac{1}{u_*^2}\overline{w^2}\frac{\partial U}{\partial z} \sim \frac{z}{u_f}\frac{1}{u_*^2}u_f^2\frac{\partial U}{\partial z} \sim 1, \tag{31}$$

resulting in

$$\frac{\partial U}{\partial z} \sim \frac{u_*}{z}\left(-\frac{z}{L}\right)^{-1/3}, \tag{32}$$

which is the same as that obtained using dimensional analysis (Carl et al. 1973). Therefore, the appropriate outer scale for $\partial U/\partial z$ is $(u_*/z_i)(-z_i/L)^{-1/3}$. We can then define the outer variable $(\partial U/\partial z)_o$ as

$$\left(\frac{\partial U}{\partial z}\right)_o = \frac{\partial U}{\partial z}\Big/\left[\frac{u_*}{z_i}\left(-\frac{z_i}{L}\right)^{-1/3}\right] = \left(\frac{z}{z_i}\right)^{-4/3} = z_o^{-4/3}. \tag{33}$$

The shear production term in Eq. (8) can then be written as

$$-\overline{uw}\frac{\partial U}{\partial z} = u_*^2\overline{uw}_o\frac{u_*}{z_i}\left(-\frac{z_i}{L}\right)^{-1/3}\left(\frac{\partial U}{\partial z}\right)_o = \frac{u_*^3}{z_i}\left(-\frac{z_i}{L}\right)^{-1/3}\overline{uw}_o\left(\frac{\partial U}{\partial z}\right)_o. \tag{34}$$

Its nondimensional form is

$$-\overline{uw}\frac{\partial U}{\partial z}\frac{z_i}{w_*^3} = \frac{u_*^3}{w_*^3}\left(-\frac{z_i}{L}\right)^{-1/3}\overline{uw}_o\left(\frac{\partial U}{\partial z}\right)_o = \left(-\frac{z_i}{L}\right)^{-4/3}\overline{uw}_o\left(\frac{\partial U}{\partial z}\right)_o. \tag{35}$$

Therefore, the small parameter ϵ in Eq. (10) is

$$\epsilon = \left(-\frac{z_i}{L}\right)^{-4/3}. \tag{36}$$

Substituting the outer expansions in Eq. (12) into Eqs. (7), (8), and (9) and collecting the terms of order ϵ, we obtain the second-order equations for the outer variables,

$$\frac{\partial \overline{w_{o,1}w_{o,2}}}{\partial \tau} = -\frac{3}{2}\frac{\partial \overline{w^2_{o,1}w_{o,2}}}{\partial z_o} + \left(\overline{p\frac{\partial w}{\partial z}}\right)_{o,2} - \left(\frac{\partial \overline{pw}}{\partial z}\right)_{o,2} + \overline{w\theta}_{o,2} - \varepsilon_{3o,12}, \tag{37}$$

$$\frac{\partial \overline{u_{o,1}u_{o,2}}}{\partial \tau} = -\overline{uw}_o\left(\frac{\partial U}{\partial z}\right)_o - \frac{\partial \overline{w_{o,1}u_{o,1}u_{o,2}}}{\partial z_o} - \frac{1}{2}\frac{\partial \overline{u^2_{o,1}u_{o,2}}}{\partial z_o} + \left(\overline{p\frac{\partial u}{\partial x}}\right)_{o,2} - \varepsilon_{1o,12}, \quad \text{and} \tag{38}$$

$$\frac{\partial \overline{\theta_{o,1}\theta_{o,2}}}{\partial \tau} = -\overline{w_{o,1}\theta_{o,2}}\left(\frac{\partial \Theta}{\partial z}\right)_o - \overline{w_{o,2}\theta_{o,1}}\left(\frac{\partial \Theta}{\partial z}\right)_o - \frac{1}{2}\frac{\partial \overline{w_{o,2}\theta_{o,1}^2}}{\partial z_o} - \frac{\partial \overline{w_{o,1}\theta_{o,1}\theta_{o,2}}}{\partial z_o} - \varepsilon_{\theta o,12}\,. \quad (39)$$

Since the first term on the right-hand side of Eq. (38) is now a leading term, we have

$$\overline{uw}_o\left(\frac{\partial U}{\partial z}\right)_o \sim \left(\overline{p\frac{\partial u}{\partial x}}\right)_{o,2} \sim \left(\overline{p\frac{\partial w}{\partial z}}\right)_{o,2} \sim \frac{\partial \overline{w_{o,1}^2 w_{o,2}}}{\partial z_o} \sim \frac{\rho_o \overline{w_{o,1}^2}\,\overline{w_{o,2}^2}^{1/2}}{z_o}, \quad (40)$$

where ρ_o is the correlation between $\overline{w_{o,1}^2}$ and $\overline{w_{o,2}^2}^{1/2}$, and $\varepsilon_{3o,12}$, $\varepsilon_{1o,12}$, and $\varepsilon_{\theta o,12}$ are the dissipation rates for $\overline{w_{o,1}w_{o,2}}$, $\overline{u_{o,1}u_{o,2}}$, and $\overline{\theta_{o,1}\theta_{o,2}}$, respectively. Here we assume that the correlation coefficient between $w_{o,1}$ and $w_{o,2}$ is also ρ_o. The fact that the pressure–strain-rate correlation terms are of the same order of magnitude and are leading terms in Eqs. (37) and (38) is used in deriving Eq. (40). In the last step the estimate $\overline{w_{o,1}^2 w_{o,2}} \sim \rho_o \overline{w_{o,1}^2}\,\overline{w_{o,2}^2}^{1/2}$ is used. Therefore, from Eqs. (33) and (25)

$$z_o^{-4/3} \sim \frac{\rho_o \overline{w_{o,1}^2}\,\overline{w_{o,2}^2}^{1/2}}{z_o}, \quad (41)$$

giving

$$\rho_o \overline{w_{o,2}^2}^{1/2} \sim z_o^{-1}. \quad (42)$$

Thus, the second-order correction term is $\overline{w_{o,1}w_{o,2}} \sim \rho_o \overline{w_{o,1}^2}^{1/2}\,\overline{w_{o,2}^2}^{1/2} \sim z_o^{-2/3}$. From Eqs. (39) and (42),

$$\frac{\overline{w_{o,2}\theta_{o,1}^2}}{z_o} \sim \frac{\overline{w_{o,1}\theta_{o,1}\theta_{o,2}}}{z_o}, \quad (43)$$

and

$$\rho_{\theta o}\overline{\theta_{o,2}^2}^{1/2} \sim z_o^{-5/3}, \quad (44)$$

where $\rho_{\theta o}$ is the correlation coefficient between $\theta_{o,1}$ and $\theta_{o,2}$. Therefore, the second-order term $\overline{\theta_{o,1}\theta_{o,2}} \sim \rho_{\theta o}\overline{\theta_{o,1}^2}^{1/2}\,\overline{\theta_{o,2}^2}^{1/2} \sim z_o^{-2}$. Thus, $\overline{w_o^2}$ and $\overline{\theta_o^2}$ with the second-order corrections for $-z/L \sim 1$ are

$$\overline{w_o^2} = \overline{w_{o,1}^2}(z_o) + 2\epsilon\overline{w_{o,1}(z_o)w_{o,2}(z_o)} + O(\epsilon^2) = A\kappa^{2/3}\left(\frac{z}{z_i}\right)^{2/3} + B\kappa^{2/3}\left(-\frac{z_i}{L}\right)^{-4/3}\left(\frac{z}{z_i}\right)^{-2/3} + O(\epsilon^2), \quad (45)$$

and

$$\overline{\theta_o^2} = \overline{\theta_{o,1}^2}(z_o) + 2\epsilon\overline{\theta_{o,1}(z_o)\theta_{o,2}(z_o)} + O(\epsilon^2) = A_\theta\left(\frac{z}{z_i}\right)^{-2/3} - B_\theta\kappa^{-2/3}\left(-\frac{z_i}{L}\right)^{-4/3}\left(\frac{z}{z_i}\right)^{-2} + O(\epsilon^2), \quad (46)$$

respectively. Rewriting the last two equations in dimensional form and dropping the $O(\epsilon^2)$ terms, we have

$$\overline{w^2} = w_*^2\overline{w_o^2} = A\kappa^{2/3}w_*^2\left(\frac{z}{z_i}\right)^{2/3} + B\kappa^{2/3}w_*^2\left(-\frac{z_i}{L}\right)^{-4/3}\left(\frac{z}{z_i}\right)^{-2/3} = Au_*^2\left(-\frac{z}{L}\right)^{2/3} + Bu_*^2\left(-\frac{z}{L}\right)^{-2/3}, \quad (47)$$

and

$$\overline{\theta^2} = \left(\frac{Q}{w_*}\right)^2\overline{\theta_o^2} = A_\theta\left(\frac{Q}{w_*}\right)^2\left(\frac{z}{z_i}\right)^{-2/3} - B_\theta\kappa^{-2/3}\left(\frac{Q}{w_*}\right)^2\left(-\frac{z_i}{L}\right)^{-4/3}\left(\frac{z}{z_i}\right)^{-2} = A_\theta\kappa^{2/3}\left(\frac{Q}{u_*}\right)^2\left(-\frac{z}{L}\right)^{-2/3} - B_\theta\left(\frac{Q}{u_*}\right)^2\left(-\frac{z}{L}\right)^{-2}, \quad (48)$$

respectively. Each of these expressions contains two nondimensional coefficients, which will be determined using measurements (section 3e). Similarly, substituting the inner expansions in Eq. (22) into Eqs. (18) and (20) and collecting the order ϵ' terms, we have the equations for the second-order inner variables,

$$\frac{1}{2}\frac{\partial \overline{w_{\text{in},1}^2}}{\partial \tau} = -\frac{3}{2}\frac{\partial \overline{w_{\text{in},1}^2 w_{\text{in},2}}}{\partial z_{\text{in}}} + \left(\overline{p\frac{\partial w}{\partial z}}\right)_{\text{in},2} - \left(\frac{\partial \overline{pw}}{\partial z}\right)_{\text{in},2} + \overline{w\theta}_{\text{in},2} - \varepsilon_{3\text{in},12}\,, \quad (49)$$

$$\frac{1}{2}\frac{\partial \overline{\theta_{\text{in},1}^2}}{\partial \tau} = -\overline{w_{\text{in},1}\theta_{\text{in},2}}\left(\frac{\partial \Theta}{\partial z}\right)_{\text{in}} - \overline{w_{\text{in},2}\theta_{\text{in},1}}\left(\frac{\partial \Theta}{\partial z}\right)_{\text{in}} - \frac{\partial \overline{w_{\text{in},1}\theta_{\text{in},1}\theta_{\text{in},2}}}{\partial z_{\text{in}}} - \frac{1}{2}\frac{\partial \overline{w_{\text{in},2}\theta_{\text{in},1}^2}}{\partial z_{\text{in}}} - \varepsilon_{\theta\text{in},12}\,, \quad (50)$$

where $\varepsilon_{3\text{in},12}$ and $\varepsilon_{\theta\text{in},12}$ are the dissipation rates for $\overline{w_{\text{in},1}w_{\text{in},2}}$ and $\overline{\theta_{\text{in},1}\theta_{\text{in},2}}$. Now the term on the left-hand side of Eq. (49) is a leading term, thus

$$\frac{\partial \overline{w_{\text{in},1}^2}}{\partial \tau} \sim \frac{\partial \overline{w_{\text{in},1}^2 w_{\text{in},2}}}{\partial z_{\text{in}}} \sim \frac{\rho_{\text{in}}\overline{w_{\text{in},1}^2}\,\overline{w_{\text{in},2}^2}^{1/2}}{z_{\text{in}}}. \quad (51)$$

In the last step the estimate $\overline{w_{\rm in,1}^2 w_{\rm in,2}} \sim \rho_{\rm in}\overline{w_{\rm in,1}^2}\,\overline{w_{\rm in,2}^2}^{1/2}$ is used, where $\rho_{\rm in}$ is the correlation between $w_{\rm in,1}^2$ and $w_{\rm in,2}^{2\,1/2}$, and we assume that the correlation coefficient between $w_{\rm in,1}$ and $w_{\rm in,2}$ is also $\rho_{\rm in}$. Therefore, from Eq. (25),

$$z_{\rm in}^{2/3} \sim \frac{\rho_{\rm in}\overline{w_{\rm in,1}^2}\,\overline{w_{\rm in,2}^2}^{1/2}}{z_{\rm in}}, \tag{52}$$

resulting in

$$\rho_{\rm in}\overline{w_{\rm in,2}^2}^{1/2} \sim z_{\rm in}^1. \tag{53}$$

Thus, the second-order correction term is $\overline{w_{\rm in,1}w_{\rm in,2}} \sim \rho_{\rm in}\overline{w_{\rm in,1}^2}^{1/2}\overline{w_{\rm in,2}^2}^{1/2} \sim z_{\rm in}^{4/3}$. From Eqs. (50) and (25),

$$\frac{\partial\overline{\theta_{\rm in,1}^2}}{\partial\tau} \sim \frac{\partial\overline{w_{\rm in,1}\theta_{\rm in,1}\theta_{\rm in,2}}}{\partial z_{\rm in}}, \tag{54}$$

and

$$\rho_{\theta\rm in}\overline{\theta_{\rm in,2}^2}^{1/2} \sim z_{\rm in}^{1/3}, \tag{55}$$

where $\rho_{\theta\rm in}$ is the correlation between $\theta_{\rm in,1}$ and $\theta_{\rm in,2}$. Therefore, the second-order term $\overline{\theta_{\rm in,1}\theta_{\rm in,2}} \sim \rho_{\theta\rm in}\overline{\theta_{\rm in,1}^2}^{1/2}\overline{\theta_{\rm in,2}^2}^{1/2} \sim z_{\rm in}^0$. Thus, $\overline{w_{\rm in}^2}$ and $\overline{\theta_{\rm in}^2}$ with the second-order corrections are

$$\begin{aligned}\overline{w_{\rm in}^2} &= \overline{w_{\rm in,1}^2}(z_{\rm in}) + 2\epsilon'\overline{w_{\rm in,1}(z_{\rm in})w_{\rm in,2}(z_{\rm in})} + O(\epsilon'^2)\\ &= A\left(-\frac{z}{L}\right)^{2/3} - C\kappa^{-2/3}\left(-\frac{z_i}{L}\right)^{-2/3}\left(-\frac{z}{L}\right)^{4/3} + O(\epsilon'^2),\end{aligned} \tag{56}$$

and

$$\begin{aligned}\overline{\theta_{\rm in}^2} &= \overline{\theta_{\rm in,1}^2}(z_{\rm in}) + 2\epsilon'\overline{\theta_{\rm in,1}(z_{\rm in})\theta_{\rm in,2}(z_{\rm in})} + O(\epsilon'^2)\\ &= A_\theta\kappa^{2/3}\left(-\frac{z}{L}\right)^{-2/3} - C_\theta\kappa^{2/3}\left(-\frac{z_i}{L}\right)^{-2/3}\left(-\frac{z}{L}\right)^{0} + O(\epsilon'^2),\end{aligned} \tag{57}$$

respectively. Rewriting the last two equations in dimensional form and dropping the $O(\epsilon'^2)$ terms, we have

$$\begin{aligned}\overline{w^2} &= u_*^2\overline{w_{\rm in}^2} = Au_*^2\left(-\frac{z}{L}\right)^{2/3}\\ &\quad - C\kappa^{-2/3}u_*^2\left(-\frac{z_i}{L}\right)^{-2/3}\left(-\frac{z}{L}\right)^{4/3}\\ &= Aw_*^2\kappa^{2/3}\left(\frac{z}{z_i}\right)^{2/3} - Cw_*^2\left(\frac{z}{z_i}\right)^{4/3},\end{aligned} \tag{58}$$

and

$$\begin{aligned}\overline{\theta^2} &= \left(\frac{Q}{u_*}\right)^2\overline{\theta_{\rm in}^2} = A_\theta\kappa^{2/3}\left(\frac{Q}{u_*}\right)^2\left(-\frac{z}{L}\right)^{-2/3}\\ &\quad - C_\theta\kappa^{2/3}\left(\frac{Q}{u_*}\right)^2\left(-\frac{z_i}{L}\right)^{-2/3}\left(-\frac{z}{L}\right)^{0}\\ &= A_\theta\left(\frac{Q}{w_*}\right)^2\left(\frac{z}{z_i}\right)^{-2/3} - C_\theta\left(\frac{Q}{w_*}\right)^2\left(\frac{z}{z_i}\right)^{0},\end{aligned} \tag{59}$$

respectively. The nondimensional coefficients in the abovementioned equations will be determined below. Summing the two asymptotic expansions and subtracting the common parts, we obtain the composite (uniform) expansions

$$\begin{aligned}\overline{w^2} &= w_*^2\left[A\kappa^{2/3}\left(\frac{z}{z_i}\right)^{2/3} + B\kappa^{2/3}\left(-\frac{z_i}{L}\right)^{-4/3}\left(\frac{z}{z_i}\right)^{-2/3} - C\left(\frac{z}{z_i}\right)^{4/3}\right]\\ &= u_*^2\left[A\left(-\frac{z}{L}\right)^{2/3} + B\left(-\frac{z}{L}\right)^{-2/3} - C\kappa^{-2/3}\left(-\frac{z_i}{L}\right)^{-2/3}\left(-\frac{z}{L}\right)^{4/3}\right],\end{aligned} \tag{60}$$

and

$$\begin{aligned}\overline{\theta^2} &= \left(\frac{Q}{w_*}\right)^2\left[A_\theta\left(\frac{z}{z_i}\right)^{-2/3} - B_\theta\kappa^{-2/3}\left(-\frac{z_i}{L}\right)^{-4/3}\left(\frac{z}{z_i}\right)^{-2} - C_\theta\left(\frac{z}{z_i}\right)^{0}\right]\\ &= \left(\frac{Q}{u_*}\right)^2\left[A_\theta\kappa^{2/3}\left(-\frac{z}{L}\right)^{-2/3} - B_\theta\left(-\frac{z}{L}\right)^{-2} - C_\theta\kappa^{2/3}\left(-\frac{z_i}{L}\right)^{-2/3}\left(-\frac{z}{L}\right)^{0}\right],\end{aligned} \tag{61}$$

which are valid in both the inner and outer layers.

e. *Comparison with measurements*

The nondimensional coefficients A, B, C, A_θ, B_θ, and C_θ are now determined using measurements from the Kansas (Wyngaard et al. 1971), Minnesota (Kaimal et al. 1976; Izumi and Caughey 1976), Atmospheric Radiation Measurement (ARM; Mather and Voyles 2013; Berg et al. 2017), and Ashchurch (Caughey and Palmer 1979) field programs. By fitting the LFC scaling term of $\overline{w^2}$ to

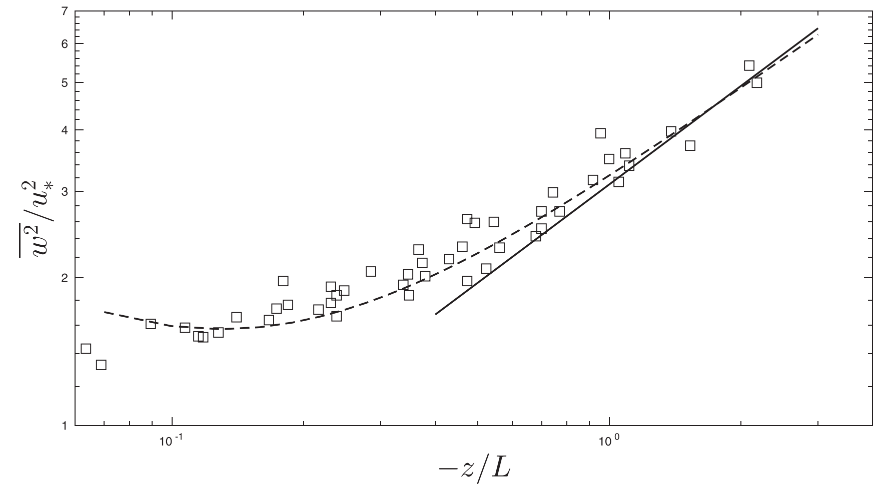

FIG. 1. Comparison of the composite expansion for the vertical velocity variance with the Kansas (1968) data in terms of the inner (surface layer) variables. The LFC limit (solid line) and LFC and the second-order correction (dashed line) are marked.

the Kansas data (Fig. 1) for $-z/L > 1$, we find $A \approx 3.1$ (the solid line in Fig. 1). Fitting Eq. (47) for $-z/L$ down to 0.1 (dashed line in Fig. 1), we obtain $B \approx 0.2$. Fitting the LFC scaling term of $\overline{\theta^2}$ to the Kansas data (Fig. 2) for $-z/L > 1$ gives $A_\theta \approx 1.8$ (the solid line in Fig. 2). Fitting Eq. (48) to the Kansas data for $-z/L$ down to 0.03 (dashed line in Fig. 2), we obtain $B_\theta \approx 0.0038$. Here the second-order corrections account for departure from the LFC scaling caused by the mean shear production for $-z/L \sim 1$. Applying the Minnesota, Ashchurch, and ARM data (Figs. 3 and 4) to Eqs. (58) and (59), we find $C \approx 1.35$ and $C_\theta \approx 1.2$. Using these values for the coefficients, the composite expansions show very good agreement with the field data. With these A and B values the expansion for $\overline{w^2}$ also fits reasonably well the Northern Hemisphere Climate Processes Land Surface Experiment (NOPEX) data (Johansson et al. 2001; not shown), which have larger scatters. For the uncertainty levels for the NOPEX data (16% for u_*^2 and 10% for z_i), it is clear from Figs. 1 and 3 that self-correlation effects do not alter the trends of the data in any significant way. Furthermore, judging from the scatter of the data points, the uncertainties in the Kansas data are lower. As a result, any effects of self-correlation would be even smaller. Therefore, the observed LFC scaling and departure from it for $-z/L \sim 1$ are due to the surface-layer physics, not self-correlation effects.

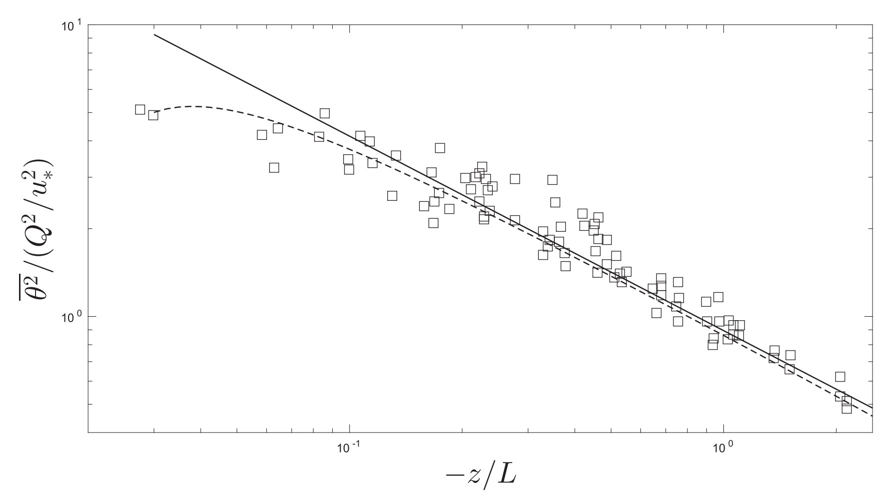

FIG. 2. Comparison of the composite expansion for the temperature variance with the Kansas (1968) data in terms of the inner (surface layer) variables. Line styles are the same as in Fig. 1.

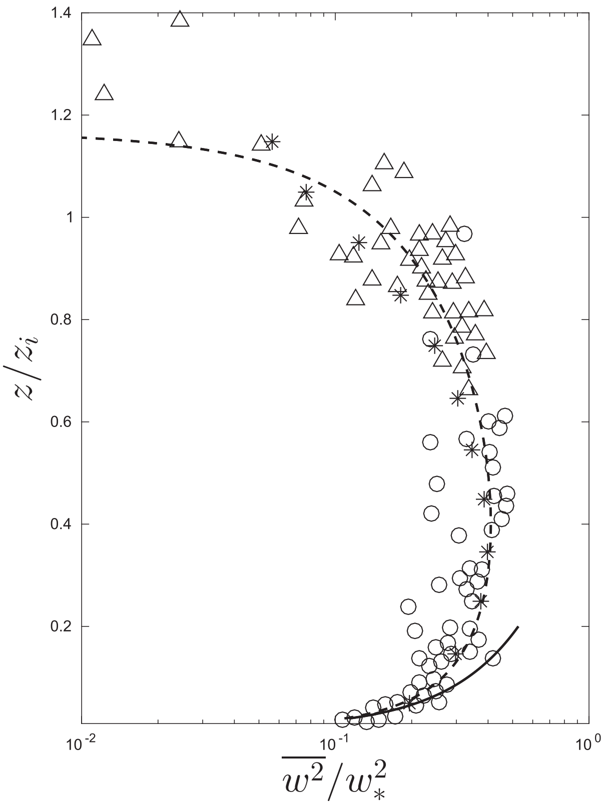

FIG. 3. Comparison of the composite expansion for the vertical velocity variance with the Minnesota (circles), Ashchurch (triangles), and ARM (asterisks) data in terms of the outer (mixed layer) variables. Line styles are the same as in Fig. 1.

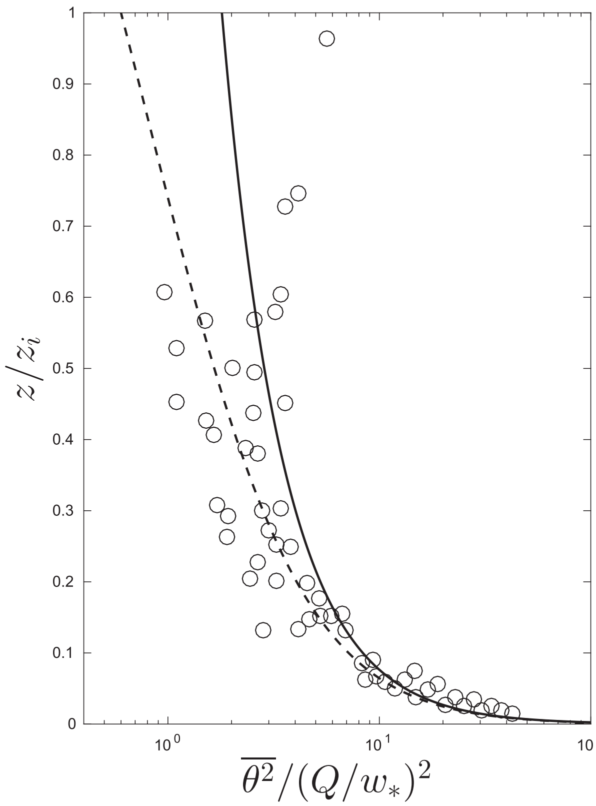

FIG. 4. Comparison of the composite expansion for the temperature variance with the Minnesota data in terms of the outer (mixed layer) variables. Line styles are the same as in Fig. 1.

The composite expansion for $\overline{w^2}$ is valid up to $z/z_i \approx 1.2$, well beyond the surface layer. Here the second-order corrections account for the influence of the inversion height (atmospheric boundary layer depth), which is reflected in the time derivative terms in Eq. (18). Unlike in the surface layer where $z/z_i \ll 1$, the turbulence is no longer in equilibrium with the external conditions (influences) when $z/z_i \sim 1$. The composite expansion for $\overline{\theta^2}$ is valid up to $z/z_i \approx 0.6$, because at the inversion layer there is a production source with different scaling, which is beyond our surface-layer analysis. From the point of view of singular perturbation problems, there is a second inner layer near $z = z_i$, which needs to be considered in the matched asymptotic expansions if we want to predict the behavior there. Therefore, the current correction cannot capture the trend of $\overline{\theta^2}$ near $z/z_i = 1$. For $\overline{w^2}$, the inversion damps the fluctuations, which does not necessarily result in a second inner layer.

The abovementioned comparisons show that by adding only the second-order corrections, the functional forms of the composite expansions already show very good agreement with the data, demonstrating the efficacy of the method of matched asymptotic expansions for analyzing the surface layer. Previously vertical profiles of turbulence statistics have been empirical expressions obtained by curve fitting field data [e.g., Caughey and Palmer (1979) for vertical velocity profiles]. Furthermore, the empirical curves for $-z/L \gtrsim 1$ and $z/z_i \lesssim 1$ are separate curves. The composite expansions obtained in the present study provide unified expressions for the vertical velocity and potential temperature variances from $-z/L \approx 0.1$ to $z/z_i \sim 1$. Equally important, each part of the expansions has a clear physical interpretation (origin).

4. Conclusions and discussions

In the reported study we used the method of matched asymptotic expansions to derive analytically Monin–Obukhov similarity theory for the vertical velocity and potential temperature variances and the local-free-convection scaling, which previously have been a hypothesis based on phenomenology. We focused on the vertical velocity and potential temperature variances.

The equations for the horizontal velocity, vertical velocity, and potential temperature variances are used to derive MOST and the LFC scaling. The dominance of buoyancy and shear production terms in the outer and inner layers, which have different scaling properties, results in a nonuniformly valid solution and a singular perturbation problem, which is solved using the method of matched asymptotic expansions. We obtained $-L$ as the thickness of the inner layer. The inner expansions were found to depend on z/L only, providing a proof of MOST for the vertical and potential temperature variances. The LFC scaling was obtained by matching the leading-order inner and outer expansions. Corrections for the departure from the scaling for $-z/L \sim 1$ and $z/z_i \sim 1$, which cannot be obtained analytically using dimensional analysis, are also derived by including the second-order expansions. The composite expansions obtained show very good agreement with the Kansas, Minnesota, Ashchurch, and Atmospheric Radiation Measurement (ARM) field data, achieved with only leading- and second-order expansions, demonstrating that matched asymptotic expansions provide an effective method for analyzing and understanding the atmospheric boundary layer.

In deriving the inner equations [Eqs. (18)–(20)], we have used the surface-layer scaling of the terms in these equations, which is supported by observational evidence (e.g., Kaimal et al. 1976; Wyngaard et al. 1971). The surface-layer scaling of these terms can also be obtained from the surface-layer similarity of multipoint statistics (Tong and Nguyen 2015), which has also been derived mathematically using the method of matched asymptotic expansions (Tong and Ding 2018). Therefore, the derived scaling in the present study is a consequence of MMO, and the derivation is mathematically rigorous. The present work is also part of a comprehensive analytical derivation of MMO and MOST.

The present study uses the balance equations for the velocity and temperature variances to derive MOST and the LFC scaling for these variables, thereby providing strong analytical support to Monin–Obukhov similarity theory. The expansions go beyond the previous observation-based empirical formulas for turbulence statistics to provide physics-based, analytically derived expressions with clear physical origins and interpretations. These expressions and the understanding of the associated physics are also potentially important for a range of applications. The vertical velocity variance is often used in eddy viscosity and diffusivity models. For example, in numerical weather prediction models using column parameterization for the boundary layer, the analytical expression for the vertical velocity profile in convective boundary layers is important for improving the predicted temperature profile under convective conditions. The derived variance profiles can also benefit prediction of atmospheric dispersion and wave propagation.

Acknowledgments. This work was supported by the National Science Foundation through Grants AGS-1335995 and AGS-1561190.

REFERENCES

Bender, C. M., and S. A. Orszag, 1978: *Advanced Mathematical Methods for Scientists and Engineers: Asymptotic Methods and Perturbation Theory.* International Series in Pure and Applied Mathematics, McGraw-Hill, 593 pp.

Berg, L. K., R. K. Newsom, and D. D. Turner, 2017: Year-long vertical velocity statistics derived from Doppler lidar data for the continental convective boundary layer. *J. Appl. Meteor. Climatol.*, **56**, 2441–2454, https://doi.org/10.1175/JAMC-D-16-0359.1.

Carl, M. D., T. C. Tarbell, and H. A. Panofsky, 1973: Profiles of wind and temperature from towers over homogeneous terrain. *J. Atmos. Sci.*, **30**, 788–794, https://doi.org/10.1175/1520-0469(1973)030<0788:POWATF>2.0.CO;2.

Caughey, S. J., and S. G. Palmer, 1979: Some aspects of turbulence structure through the depth of the convective boundary layer. *Quart. J. Roy. Meteor. Soc.*, **105**, 811–827, https://doi.org/10.1002/qj.49710544606.

Cousteix, J., and J. Mauss, 2007: *Asymptotic Analysis and Boundary Layers.* Scientific Computation, Springer-Verlag, 434 pp., https://doi.org/10.1007/978-3-540-46489-1.

Haugen, D. A., J. C. Kaimal, and E. F. Bradley, 1971: An experimental study of Reynolds stress and heat flux in the atmospheric surface layer. *Quart. J. Roy. Meteor. Soc.*, **97**, 168–180, https://doi.org/10.1002/qj.49709741204.

Izumi, Y., and J. S. Caughey, 1976: Minnesota 1973 Atmospheric Boundary Layer Experiment data report. Air Force Cambridge Research Laboratories Tech. Rep. AFCRL-TR-0038, Environmental Research Papers 547, 28 pp.

Johansson, C., A.-S. Smedman, U. Högström, J. G. Brasseur, and S. Khanna, 2001: Critical test of the validity of Monin–Obukhov similarity during convective conditions. *J. Atmos. Sci.*, **58**, 1549–1566, https://doi.org/10.1175/1520-0469(2001)058<1549:CTOTVO>2.0.CO;2.

Kaimal, J. C., J. C. Wyngaard, D. A. Haugen, O. R. Coté, Y. Izumi, S. J. Caughey, and C. J. Readings, 1976: Turbulence structure in the convective boundary layer. *J. Atmos. Sci.*, **33**, 2152–2169, https://doi.org/10.1175/1520-0469(1976)033<2152:TSITCB>2.0.CO;2.

Mather, J. H., and J. W. Voyles, 2013: The ARM Climate Research Facility: A review of structure and capabilities. *Bull. Amer. Meteor. Soc.*, **94**, 377–392, https://doi.org/10.1175/BAMS-D-11-00218.1.

Monin, A. S., and A. M. Obukhov, 1954: Basic laws of turbulent mixing in the ground layer of the atmosphere. *Tr. Geofiz. Inst., Akad. Nauk SSSR*, **24**, 163–187.

Obukhov, A. M., 1946: Turbulence in the atmosphere with inhomogeneous temperature. *Tr. Inst. Teor. Geofiz., Akad. Nauk SSSR*, **1**, 95–115.

Tennekes, H., 1970: Free convection in the turbulent Ekman layer of the atmosphere. *J. Atmos. Sci.*, **27**, 1027–1034, https://doi.org/10.1175/1520-0469(1970)027<1027:FCITTE>2.0.CO;2.

Tong, C., and K. X. Nguyen, 2015: Multipoint Monin–Obukhov similarity and its application to turbulence spectra in the convective atmospheric surface layer. *J. Atmos. Sci.*, **72**, 4337–4348, https://doi.org/10.1175/JAS-D-15-0134.1.

Van Dyke, M., 1975: *Perturbation Methods in Fluid Mechanics.* The Parabolic Press, 271 pp.

Wyngaard, J. C., and O. R. Coté, 1971: The budgets of turbulent kinetic energy and temperature variance in the atmospheric surface layer. *J. Atmos. Sci.*, **28**, 190–201, https://doi.org/10.1175/1520-0469(1971)028<0190:TBOTKE>2.0.CO;2.

——, ——, and Y. Izumi, 1971: Local free convection, similarity, and the budgets of shear stress and heat flux. *J. Atmos. Sci.*, **28**, 1171–1182, https://doi.org/10.1175/1520-0469(1971)028<1171:LFCSAT>2.0.CO;2.